Electrochemical and optical characterization of *p*- and *n*-doped poly[2-methoxy-5-(2-ethylhexyloxy)-1,4-phenylenevinylene]

A. L. Holt, J. M. Leger, and S. A. Carter[a)]
Department of Physics, University of California, Santa Cruz, California 95064

(Received 9 March 2005; accepted 16 May 2005; published online 2 August 2005)

We study electrochemical *p*- and *n*-type doping in the well-known light-emitting polymer poly[2-methoxy-5-(2-ethylhexyloxy)-1,4-phenylenevinylene] (MEH-PPV). Doping reactions are characterized using cyclic voltammetry. Optical measurements including photoluminescence and UV/Vis/NIR transmission were performed on doped samples. We find that oxidation in MEH-PPV is a highly reversible reaction resulting in stable freestanding doped films, while the reduced form is unstable and the reaction irreversible. We discuss the dependence of doping reactions on scan rate, film thickness, salt type and concentration, and working electrode type. We observe the development of two additional broad absorption bands in both lightly and heavily doped films accompanied by a slight blueshift in the primary optical transition, suggesting bipolaron band formation. Finally we find that both *p* and *n* dopings result in extremely sensitive photoluminescence quenching. We propose a physical model for understanding electrochemical doping in MEH-PPV and the implications this has on the development of such technologies as polymer light-emitting electrochemical cells, electrochromic devices, actuators, and sensors. © *2005 American Institute of Physics*. [DOI: 10.1063/1.1949188]

I. INTRODUCTION

The soluble derivatives of poly(phenylenevinylene) (PPV) are useful for studying the mechanical and electrical characteristics of luminescent, conducting polymers. One of the most well studied soluble PPV derivatives is poly[2-methoxy-5-(2-ethylhexyloxy)-1,4-phenylenevinylene] (MEH-PPV). Commended for its ease of use, reproducibility, and versatility, MEH-PPV is widely used in the study of many applications such as organic polymer photovoltaics,[1] light-emitting diodes[2–4] and light emitting electrochemical cells (LECs),[5,6] as well as a water soluble version in biosensor application.[7] In recent work, MEH-PPV was the material of choice for a solid-state electrochromic device because of the sharp contrast in color between doped and undoped states.[8]

Understanding the factors affecting doping reactions and the effects that doping have on the characteristics of the polymers are essential to the improvement of existing technologies in which doping is a critical component of the operating mechanism such as LECs,[9,10] piezoelectric devices,[11] and electrochromic devices.[12,13] That knowledge is equally valuable for application to the development of novel technologies such as in biosensors, and integrated sensors and displays.

The doping process in conducting polymers as currently understood introduces deformations called solitons, polarons, and bipolarons into the polymer system causing new levels to form in the band gap, increasing the amount of possible energy transitions.[14,15] Because polymers are inherently disordered, it is difficult to characterize the fundamental roles of these quasiparticles in the doping process. Many optical spectroscopic techniques are used to explore doping in conducting polymers. We can better understand the dopant deformations by utilizing these experimental techniques as well as by studying theoretical models.

There have been many studies on the electrochemistry of PPV and on the optical properties of doped PPV using Raman spectroscopy,[16–18] UV absorption, and infrared absorption[19] as well as many studies on the electronic and electrochemical properties of PPV and its derivatives.[20–23] Despite the importance of MEH-PPV in devices, studies on the electrochemical and optical characteristics of doped MEH-PPV (Ref. 24) have been fairly limited in scope.

In this paper, we present an electrochemical study of the *p*- and *n*-doping processes in MEH-PPV, and its affect on the absorption and photoluminescence spectra of the polymer. Different methods were used to analyze the doping process of MEH-PPV. Cyclic voltammetry is used to characterize and study redox reactions at an electrode with regard to such properties as reversibility, stability, and doping onset values. UV/VIS/NIR transmission spectra and photoluminescence spectra were obtained in order to examine the changes in optical transitions associated with *p*- and *n*- type doping in MEH-PPV. This information is vital, for example, to the development of optical sensors in which photoluminescence quenching is the determining factor.

II. EXPERIMENT

The polymer studied was MEH-PPV provided by American Dye Source. MEH-PPV is an orangish-red colored, luminescent polymer easily solvable in common organic solvents that exhibits a color change to greenish brown when

[a)]Electronic mail: sacarter@ucsc.edu

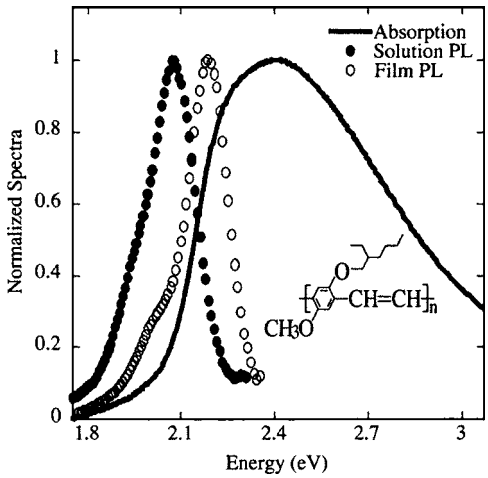

FIG. 1. MEH-PPV chemical structure, absorbtance spectra, and photoluminescence spectra for the film and solution.

electrochemically doped. Figure 1 shows the structure and absorption and photoluminescence spectra of MEH-PPV.

Cyclic voltammetry experiments were performed using a nonaqueous silver/silver ion reference electrode [Ag/Ag^+, 0.3 V versus standard calomel electrode (SCE)], a platinum counterelectrode and most often, a MEH-PPV/indium tin oxide (ITO) working electrode. Other working electrodes tested were MEH-PPV/gold, aluminum, and titanium nitride (TiN). The substrates consisted of ITO glass substrates, provided by Thin Film Devices, TiN substrates,[25] and metals, such as gold, aluminum, and silver, thermally deposited up to 50 nm on glass. A polymer solution of MEH-PPV and chlorobenzene was then spun cast on the metal to the desired thickness. Following polymer deposition, all substrates were annealed at 120 °C for 1 h under vacuum and dried in a vacuum chamber overnight. The electrolyte consisted of salts of lithium trifluoromethanesulfonate (Li triflate), tetrabutylammonium tetrafluoroborate (TBA BF_4), or TBA triflate in acetonitrile at 0.01*M* and was purged with nitrogen prior to testing in order to reduce oxygen contamination. Data were obtained on an EG&G Princeton Applied Research model 362 scanning potentiostat and two 2010 Keithley multimeters. Film thickness measurements were taken using a Thermomicroscope Autoprobe CP atomic force microscope and typically have a variation of ~15%.

The transmission spectra for *p*-doped films were taken on three machines each with a different wavelength range to study the material from the visible region past the near infrared region. For wavelengths from 380 to 1200 nm, transmission spectra were taken with a Perkin Elmer UV/Vis/NIR spectrometer Lambda 9 and for the *in situ n*-doped films, with a Varian Cary 3 spectrophotometer. A Perkin Elmer Spectrum One spectrometer was used for the range from 1100 to 3000 nm. Although the data from each machine matched fairly well, to neatly plot the full range for the *p*-doped films, data from the Spectrum One were shifted by no more than 6% of the total absorption to match that from the Lambda 9 in the overlap region between 1100 and 1200 nm. The photoluminescence spectra were acquired only on the *p*-doped films using a Perkin Elmer luminescence spectrometer LS 45. The material was excited at 505 nm, the undoped MEH-PPV absorption maximum. Solid-state devices for photoluminescence and absorption experiments were constructed as described previously.[8]

For optical studies of *p*-doped MEH-PPV, removing films from the electrolyte solution at the desired doping voltage produced films of different doping levels. The *p*-doped films retained their characteristics indefinitely. However, optical spectra of *n*-doped MEH-PPV films were more difficult to acquire as *n*-doped films are highly unstable. They must be kept under constant potential and cannot be removed from the electrolyte. Thus, *in situ* experiments were performed solely on one instrument in a wavelength range from 380 to 900 nm. The stability of the doped samples depends on exposure to air and thus would have been improved by performing all experiments in an inert atmosphere.

III. RESULTS AND DISCUSSION

A. Cyclic voltammetry

Cyclic voltammetry was the primary tool used to characterize doping in MEH-PPV and was also used to produce doped films for transmission and photoluminescence studies. In the redox reactions of a MEH-PPV film, counterions from the electrolyte diffuse into the material and allow the *p* and *n* doping of the material. MEH-PPV is capable of being both *p* and *n* doped and exhibits a color change from orangish red to greenish brown.[24] With *p* doping, the anodic peak occurs at about 0.8 V (vs Ag/Ag^+) and the cathodic peak at about 0.4 V. For voltages higher than 1 V, increases in the current indicate the onset of an overoxidation peak that occurs around 1.3 V and results in the degregation of the polymer. We performed experiments exploring the effects that the salt type and salt concentration in the electrolyte have on the doping process as well as how the doping of the material is affected by the working electrode type, the scan rate, and the film thickness.

Anions tested in the *p*-doping process were triflate$^-$, tetrafluoroborate (BF_4^-), hexafluorophosphate (PF_6^-), and sulfonate (SO_4^-). When examining the optical contrasts in solid-state devices, we observed that organic anions were slightly more effective at *p* doping than inorganic ones.[8] In the cyclic voltammetry experiment, however, no systematic differences were observed for the different salts. This could be due to larger errors in the cyclic voltammetry experimental setup or due to varying mobilities of ions in the solid electrolyte of the solid-state devices.

Cations tested in the *n*-doping process were Li^+ and TBA^+. It has been demonstrated that alkaline cations cannot effectively electrochemically *n* dope polythiophene or polyacetylene in certain solvents such as acetonitrile and propylene carbonate due to their small effective ionic radius.[26,27] The cyclic voltammogram in Fig. 2 shows that there is no redox reaction in the negative voltage range, suggesting that Li^+ is unable to *n* dope MEH-PPV. Only slightly reversible *n* doping accompanied by color change occurs with the organic cation TBA^+. It is understood that most polymers are electrochemically unstable when *n* doped due to redox reactions

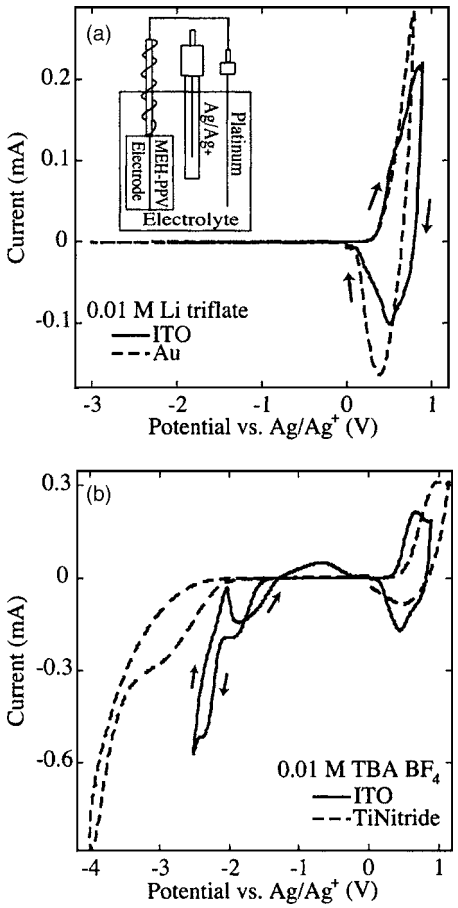

FIG. 2. Cyclic voltammetry setup and cyclic voltammograms for various MEH-PPV working electrodes with (a) 0.01*M* Li triflate and (b) 0.01*M* TBA BF_4 electrolyte.

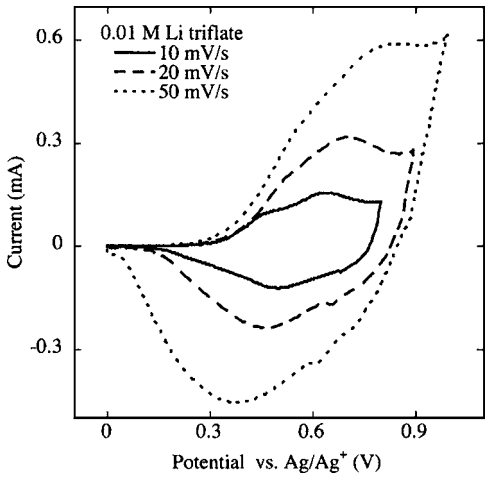

FIG. 3. Cyclic voltammogram for MEH-PPV at varied scan rates in 0.01*M* Li triflate electrolyte.

with water and oxygen.[28] An indication of the instability of *n*-doped MEH-PPV was its inability to retain a change in color outside of the electrolyte.

Under a carefully monitored experimental setup, the highest occupied molecular-orbital (HOMO) and the lowest unoccupied molecular-orbital (LUMO) energy levels of a conductive polymer can be approximated by the *p*- and *n*-doping onset potentials.[29] We performed detailed studies on whether the electrodes, ITO, Au, Ag, Al, and TiN, onto which the polymer is deposited affect the onset potentials. The onset potentials for *n* and *p* dopings, determined from the intercept of a line tangent to half the largest slope value, for most of the electrodes varied no more than 0.05 eV and suggest an electrochemical band gap of about 2.4 eV, corresponding well with previous studies of single-particle energy gaps at 2.45 eV.[30] This is expected due to the insensitivity of the onset potentials to the work function of the electrode. Using the methods employed by Li *et al.*[29] to calculate the HOMO and LUMO levels for MEH-PPV, the average level for the HOMO was about −5.1 eV and for the LUMO, −2.7 eV. These values, listed in Table I for various electrode materials, are similar to those calculated by Li *et al.*[29] and Cervini *et al.*[22]

In general, for a Nerstian system, a reversible redox reaction meets the criteria that the peak potentials are independent of the sweep rate with a difference of 54 mV between them and that the ratio of the current values at the peak potentials is unity. The redox reaction of MEH-PPV is a quasireversible one. This is illustrated in Fig. 3 which shows that for higher scan rates, the anodic peak occurs at a higher potential and the current increases. The increase in current for faster scan rates is a result of charge conservation while the increase in anodic peak potential indicates that the rate of reaction is comparable to the scan rate.

The reversibility of MEH-PPV depends on which type of metal is used for the electrode. As depicted in Fig. 2, for

TABLE I. Doping onset potentials, calculated HOMO/LUMO levels, electrochemical band gap, and qualitative reversibility for MEH-PPV on various electrodes.

Electrode	*p* onset (V)[a]	*n* onset (V)[a]	HOMO (eV)[b]	LUMO (eV)[b]	Electrochemical band gap (eV)[c]	Reversibility[d]
ITO	0.32	−2.10	−5.02	−2.60	2.42	*n* and *p*
Au	0.34	−2.00	−5.04	−2.70	2.34	*n* and *p*
TiN	0.49	−2.00	−5.19	−2.70	2.49	Slightly in *n*
Ag	0.31	−2.00	−5.01	−2.70	2.31	*n* only
Al	0.60	−2.66	−5.30	−2.04	3.26	Slightly in *n*

[a] $V_{error} \pm 0.05$ V.
[b] $eV_{error} = \pm 0.05$ eV.
[c] $eV_{error} = \pm 0.1$ eV.
[d] As determined by the visible color change.

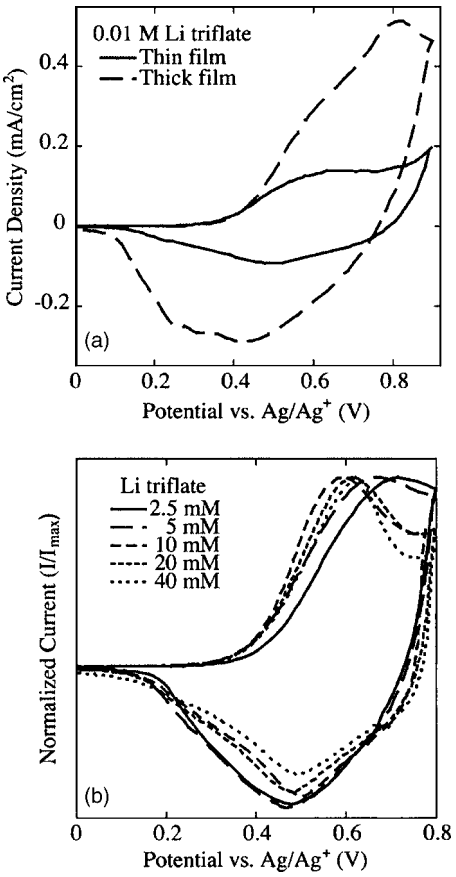

FIG. 4. Cyclic voltammograms for MEH-PPV for (a) different film thicknesses and (b) varied salt concentration.

p doping using TiN, the cathodic peak has a much lower current value than the anodic peak in contrast to ITO and Au which both have more comparable peak heights. When *n* doping, reversibility is higher for the ITO electrode than TiN which has no anodic peak. We assign the second peak at −2.5 V for ITO as the cathodic peak for *n* doping of MEH-PPV and assign the first peak to the reduction of ITO.

The difference in reversibility for the various electrodes may be due to the oxidation of Al and Ag, resulting in a nonuniform color change of the film. No anodic peaks were observed with *p* doping for Ag and Al, only overoxidation onset and they exhibited a color change reaction with small increasing fully doped regions that afterwards failed to return to their original color. It is possible that an oxide layer formed on the metal prevents the uniform doping of the polymer material. The *n*-doping reactions, however, were slightly more reversible but showed similar features.

Although the doping onset potentials should not be affected by the experimental setup, the position of the doping current peaks are affected by salt concentration in the electrolyte and film thicknesses. Increasing salt concentration in the electrolyte increases the reaction rate and occurs until the effects of ion pairing in the concentrated electrolyte slow the reaction rate down.[8] This affects the anodic and cathodic peak potentials and is the opposite effect to that of increasing the film thickness. Due to reduced ion mobility, a thicker film exhibits a slower reaction rate. Figure 4 exhibits the effects

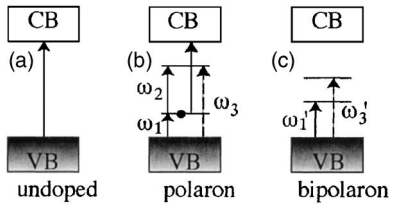

FIG. 5. Illustration of the energy transitions for (a) an undoped polymer, (b) a positive polaron, and (c) a positive bipolaron.

that film thickness and salt concentration have on the anodic and cathodic peak positions. It should be noted that the onset potentials, however, remain constant.

B. Absorption progression

Terms frequented when discussing the doping of organic conducting polymers with nondegenerate ground states are polaron and bipolaron. These terms describe localized charge distributions that accompany a distortion in the polymer chain. This lattice relaxation stretches over many repeat units. Polarons and bipolarons are considered quasiparticles because they are mobile on the polymer chain. Upon oxidation, an electron is removed from the pi system of the polymer backbone, leaving a positive spinless charge and a free radical. This spin $\frac{1}{2}$ combination, called a polaron, creates two energy levels inside the band gap, one singly occupied, symmetrically placed around the center of the gap. That single electron can also be removed creating a spinless bipolaron with localized energy states farther from the band edges than the polaron states because of the stronger lattice relaxation. Figure 5 displays the energy levels of these quasiparticles as well as the possible energetic transitions. Within the continuum electron-phonon-coupled model utilized by Fesser, Bishop, and Campbell (FBC model), ω_1 and ω_2 are the dominant transitions for the polaron and ω_1' for the bipolaron.[31]

Theories and past experiments suggest that polarons are present in systems at low doping levels while bipolarons are more favorable at higher doping levels.[32] As shown in Fig. 6, we examine the absorption spectra of MEH-PPV and observe two midgap transitions at high doping voltages, at about 1.74

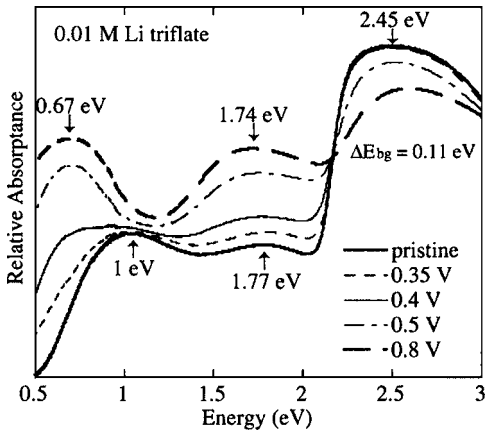

FIG. 6. Absorptance spectra for a MEH-PPV film at progressive doping levels.

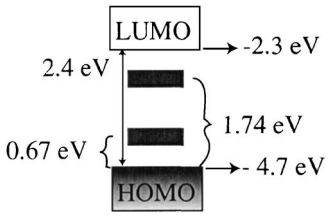

FIG. 7. Illustration of bipolaron energy levels in MEH-PPV.

and 0.67 eV, consistent with the theory of bipolaron formation. Figure 7 depicts these transitions with $\omega_1'=0.67$ eV and $\omega_3'=1.74$ eV which sum up to approximately equal the band gap which peaks at about 2.45 eV. We observe a shift in spectral weight from the band-gap transition to the ω_1' and ω_3' bipolaron transitions as expected. We also observe a blueshift of about 0.11 eV in the interband absorption peak that accompanies the extremely broad low-energy transition, indicating the formation of bipolaron bands within the gap that occurs with heavy doping.[14] Within the FBC model, the absorption coefficient and confinement parameter are both functions of the ratio ω_0/Δ_0 where $\omega_0=(\omega_3'-\omega_1')/2$ for bipolarons and $\Delta_0=E_g/2$. For MEH-PPV, the ratio $\omega_0/\Delta_0=0.44$ and is consistent with previous measurements.[20] However, the ratio of the intensities of the two peaks $I(\omega_1')/I(\omega_3')=I(0.67\text{ eV})/I(1.74\text{ eV})=1$ does not agree with $I(\omega_1')/I(\omega_3')\approx 12$ as predicted by the FBC model. The "intensity anomaly" has been frequently discussed and justified with ideas such as theoretical drawbacks within the FBC model and misallocated transitions.

Also inconsistent with the polaron/bipolaron picture is the observation of only two transitions in addition to the primary transition at low doping levels. As the doping level increases, the lower-energy transition at 1 eV disappears while the higher-energy one at 1.77 eV appears to either redshift at 0.03 eV or be replaced by a different optical transition at 1.74 eV. Since both transitions appear in the pristine spectra as well as at lower doping levels, there may be other reasons for their appearance. The 1-eV transition is likely caused by a doping reaction between ITO and the MEH-PPV film as it is not present when the spectra are obtained on quartz while the higher-energy transition tends to be more prominent in thinner films and are likely due to aggregation in the polymer film.

The most favorable defect with doping and its depiction in electron spin resonance (ESR), Raman, and absorption data is currently in debate. Theoretically, models using the Su–Schrieffer–Heeger model Hamiltonian[33,34] find bipolarons to be more energetically favorable due to the greater lattice relaxation, while others[35] which consider electron-electron interactions find that because of Coulomb interactions, polarons are energetically more stable until high doping levels are reached where bipolarons are formed. Many initial experimental investigations concluded that polarons were present in lightly doped systems followed by bipolaron formation with greater doping confirmed by observed optical transitions and ESR studies.[35,32] The intensities of the optical transitions though did not agree with the intensity relationships proposed by the FBC model. More recently,

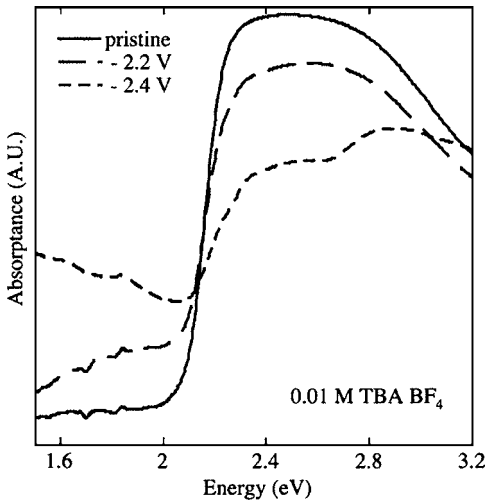

FIG. 8. *In situ* obtained absorbtance spectra of an *n*-doped MEH-PPV film.

Furukawa[36] who reassigned observed transitions to remedy the intensity anomaly argued that polarons are the primary doping species in nondegenerate polymers and the ESR results are due to polaron–polaron interactions. However, the energy transition reassignments do not add up to the interband transition. Others using vibrational spectroscopy have come to the conclusion that polarons and bipolarons are both present in thermal equilibrium at high doping levels.[16,17] Still others suggest that two transitions correspond to polarons and one transition corresponds to bipolarons and that previous doping levels were not high enough to detect the single transitions associated with bipolarons.[37] Our data suggest primarily bipolaron formation and bipolaron band formation at heavy doping levels because of the values of the energy levels. It is a possibility that we are observing the coexistence of polarons and bipolarons at heavy doping because of the inability to distinguish several specific transitions within the broad low-energy transition peak. In that case, vibrational spectroscopy would be needed to distinguish the two.

We also performed limited range *in situ* absorption experiments in order to obtain spectra for *n*-doped MEH-PPV films. Using MEH-PPV/ITO as the working electrode, we observe reversible *n*-doping reactions. Figure 8 shows the spectral progression and a color change is evident. There is a decrease in the intensity of the interband transition peak accompanied by an increase in the intensity of absorption at lower energies for doping voltage values up to −2.4 V. Larger negative voltages applied across the material resulted in *n*-doped films of greater instability and the data acquired provided no new information. We see an additional peak forming with a higher spectral weight at 2.9 eV likely caused by changes in the absorption spectra of *n*-doped ITO. There also appears to be a peak forming between 1 and 1.5 eV; however, this is not certain due to the limited energy range.

C. Photoluminescence quenching

As MEH-PPV is doped, color change is preceded by a quenching effect in the photoluminescence of the material. Figure 9 shows that for *p* doping, the photoluminescence is

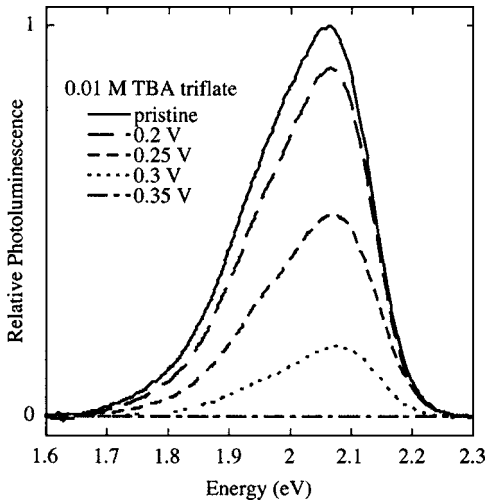

FIG. 9. Photoluminescence spectra for MEH-PPV film at progressive oxidation levels.

entirely quenched at 0.35 V while visually, color change typically occurs at about 0.5 V. Similarly, photoluminescence (PL) quenching in reverse bias (performed *in situ* due to inherent instability) is quenched fully at around −2.2 V as shown in Fig. 10. Similar degrees of photoluminescence quenching with doping occur in the solid-state devices as well and the photoluminescence is fully recovered upon dedoping. Photoluminescence quenching is expected for doped MEH-PPV because as the material becomes more metallic, there are more states available to which an exiton can nonradiatively decay. Photoluminescence quenching due to electrochemical doping has been observed in polythiophene films[38] and similar effects due to photo-oxidation have been observed in PPV films[39] and MEH-PPV solution.[40] The sensitivity of the photoluminescence spectra to doping level is likely due to the observation that the effective size of the defect is much larger than its actual size for trapping exitons and one defect is able to quench an entire polymer chain.[41]

An interesting effect occurs when attempting to *n* dope the solid-state devices. When using Li triflate, the photoluminescence of the material increases by up to 50% with increasingly negative voltages down to −3 V. It is possible that prior to testing, there are already defect sites in the polymer film from reactions with ITO, as studied by Werner *et al.*[42] The application of a voltage across the pristine device aids in the removal of these impurities from the material, thereby increasing its ability to photoluminescence. When performing the same experiment in the absence of salt, the PL again increases, but to a lesser degree, indicating the presence of charged mobile defects that can be pulled from the film. The more pronounced effect seen in the devices with salt indicates either that anions initially present in the films contribute to a limited amount of PL quenching, or that some PL quenching caused by the ITO defects is able to be compensated by the introduction of cations. At higher doping voltages, no resulting *n* doping occurred as expected for Li triflate. On the other hand, when using TBA triflate, initially the photoluminescence increases as with Li triflate but thereafter proceeds to decrease slowly, indicating the occurrence of moderate *n* doping in the polymer layer.

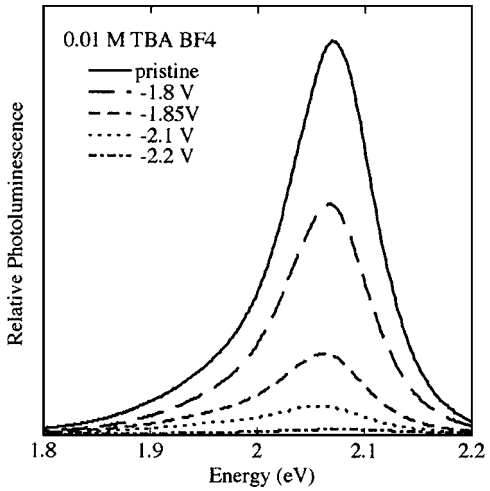

FIG. 10. Photoluminescence spectra for MEH-PPV film at progressive reduction levels.

IV. CONCLUSIONS

The electrochemical properties and doping processes of MEH-PPV, a useful light-emitting soluble derivative of PPV, were extensively studied and the results of the cyclic voltammetry experiments, absorption studies, and photoluminescence studies were presented. Cyclic voltammetry curves of MEH-PPV illustrate the dependence of the doping process on salt type, salt concentration, film thickness, and electrode type. Although the type of salt used has little effect on the process, the quasireversible doping reaction of MEH-PPV is susceptible to changes in salt concentration and film thickness which affect the speed of the reaction. Theoretically, electrode type should not affect the doping onset potentials, as they reflect the HOMO and LUMO levels of the polymer but not the work function of the electrode. This was observed for the most part in agreement with other experimental studies. However, oxygen sensitivity does affect the onset potentials for electrodes Al and TiN. Throughout the doping process, transmission and photoluminescence spectra were taken. The absorption spectra indicate the formation of bipolarons with heavy doping. Other transitions observed at low doping levels were attributed to aggregation and reactions with the substrate ITO. *In situ* transmission and photoluminescence data were obtained for *n*-doped MEH-PPV films which have not before been published or studied. Photoluminescence in MEH-PPV was much more sensitive to doping level than the absorption and was observed to be almost entirely quenched prior to the visible color change for both *p*- and *n*-doped materials in agreement with observations that one defect is able to create a quenching site the size of an entire chain.

ACKNOWLEDGMENTS

We gratefully acknowledge support from NSF ECS Grant No. 0101794. The authors wish to thank Dr. Luisa Bozano of IBM for assistance with the NIR transmission measurements.

[1] G. Yu, C. Zhang, and A. J. Heeger, Appl. Phys. Lett. **64**, 1540 (1994).
[2] R. H. Friend, R. W. Gymer, A. B. Holmes *et al.*, Nature (London) **397**, 539 (1990).
[3] D. Braun and A. J. Heeger, Thin Solid Films **216**, 96 (1992).
[4] I. D. Parker, J. Appl. Phys. **75**, 1656 (1994).
[5] L. F. Santos, L. M. Carvalho, F. E. G. Guimaraes, D. Goncalves, and R. M. Faria, Synth. Met. **121**, 1697 (2001).
[6] Y. Yang and Q. Pei, Appl. Phys. Lett. **68**, 2708 (1996).
[7] L. Chen, D. W. McBranch, H. Wang, R. Helgeson, F. Wudl, and D. Whitten, Proc. Natl. Acad. Sci. U.S.A. **96**, 12287 (1999).
[8] A. L. Holt, J. M. Leger, and S. A. Carter, Appl. Phys. Lett. **86**, 123504 (2005).
[9] Q. Pei, G. Yu, C. Zhang, Y. Yang, and A. J. Heeger, Science **269**, 1086 (1995).
[10] Q. Pei, Y. Yang, G. Yu, C. Zhang, and A. J. Heeger, J. Am. Chem. Soc. **118**, 3922 (1996).
[11] E. Fukada, IEEE Trans. Ultrason. Ferroelectr. Freq. Control **47**, 1277 (2000).
[12] P. M. S. Monk, R. J. Mortimer, and D. R. Rosseinsky, *Electrochromism: Fundamentals and Applications* (VCH, Weinheim, 1995).
[13] R. Mortimer, Electrochim. Acta **44**, 2971 (1999).
[14] J. L. Bredas and G. B. Street, Acc. Chem. Res. **18**, 309 (1985).
[15] D. Baeriswyl, D. Campbell, and S. Mazumdar, in *Conjugated Conducting Polymers*, edited by H. Kiess (Springer, Berlin, 1992), pp. 36–46; *ibid.*, pp. 191–195.
[16] M. Baitoul, J. Wery, J. P. Buisson, G. Arbuckle, H. Shah, S. Lefrant, and M. Hamdoume, Polymer **44**, 6955 (2000).
[17] M. Bairoul, J. P. Buisson, S. Lefrant, B. Dulier, J. Wery, and M. Lapkowski, Synth. Met. **84**, 623 (1997).
[18] J. Obrzut and F. E. Karasz, J. Chem. Phys. **87**, 6178 (1987).
[19] A. Sakamoto, Y. Furukawa, and M. Tasumi, J. Phys. Chem. **98**, 4635 (1994).
[20] K. F. Voss, C. M. Foster, L. Smilowitz *et al.*, Phys. Rev. B **43**, 5109 (1991).
[21] H. Eckhardt, L. W. Shacklette, K. Y. Jen, and R. L. Elsenbaumer, J. Chem. Phys. **91**, 1303 (1989).
[22] R. Cervini, X. C. Li, G. W. C. Spencer, A. B. Holmes, S. C. Moratti, and R. H. Friend, Synth. Met. **84**, 359 (1997).
[23] I. Orion, J. P. Buisson, and S. Lefrant, Phys. Rev. B **57**, 7050 (1998).
[24] L. F. Santos, L. Gaffo, L. M. De Carvalho, D. Goncalves, and R. M. Faria, Mol. Cryst. Liq. Cryst. Suppl. Ser. **374**, 469 (2002).
[25] Information provided upon request.
[26] G. Zotti, G. Schiavon, and S. Zecchin, Synth. Met. **72**, 275 (1995).
[27] M. Mastrogostino and L. Soddu, Electrochim. Acta **35**, 463 (1990).
[28] D. M. de Leuw, M. M. J. Simenon, A. R. Brown, and R. E. F. Einerhand, Synth. Met. **87**, 53 (1997).
[29] Y. Li, Y. Cao, J. Gao, D. Wang, G. Yu, and A. Heeger, Synth. Met. **99**, 243 (1999).
[30] I. H. Campbell, T. W. Hagler, and D. L. Smith, Phys. Rev. Lett. **76**, 1900 (1996).
[31] K. Fesser, A. R. Bishop, and D. K. Campbell, Phys. Rev. B **27**, 4804 (1983).
[32] A. O. Patil, A. J. Heeger, and F. Wudl, Chem. Rev. (Washington, D.C.) **88**, 183 (1988).
[33] W. P. Su, J. R. Schrieffer, and A. J. Heeger, Phys. Rev. B **22**, 2209 (1980).
[34] Y. Shimoi and S. Abe, Phys. Rev. B **50**, 14781 (1994).
[35] J. L. Bredas, J. C. Scott, K. Yakushi, and G. B. Street, Phys. Rev. B **30**, 1023 (1984).
[36] Y. Furukawa, J. Phys. Chem. **100**, 15644 (1996).
[37] J. J. Apperloo, J. van Haare, and R. Janssen, Synth. Met. **101**, 417 (1999).
[38] S. Hayashi, K. Kaneto, and K. Yoshino, Solid State Commun. **61**, 249 (1987).
[39] M. Yan, L. J. Rothberg, F. Papadimitrakopoulos, M. E. Galvin, and T. M. Miller, Phys. Rev. Lett. **73**, 744 (1994).
[40] S. Li, F. Xiong, H. Zhang, X. Lu, L. Yi, and G. Yang, Chin. J. Chem. **22**, 80 (2004).
[41] D. Vanden Bout, W. Yip, D. Hu, D. Fu, T. Swager, and P. Barbara, Science **277**, 1074 (1997).
[42] E. Werner, M. Meier, J. Gmeiner, M. Herold, W. Brutting, and M. Schwoerer, Opt. Mater. (Amsterdam, Neth.) **9**, 109 (1998).